コンクリート工学年次論文報告集, Vol.15, No. 2, 1993

論 文

[2213] An Experimental Study on Joint Strength of Spliced Bars for Precast Concrete Structures

Rodolfo YANEZ*1, Ken TABATA*2, Teruaki YAMAGUCHI*3,

and Hiroshi IMAI*4

1. INTRODUCTION

During an earthquake, the stresses at the end of the structural members become larger, therefore it is desirable for the bar joints of Precast Concrete (PCa) structures to be placed at the less stressed portion of beams and columns, to ensure satisfactory strength and ductility against seismic forces.

The bar joint method proposed by Imai et. al. [1], [2] was proved to be good enough to transfer the stresses from each bar to the surrounding concrete matrix. However, it is a fact that as the bar diameter increases the resistant surface of concrete to the splitting force becomes smaller and the bond strength decreases. In the proposed system a steel sheath with diameters of 42 mm has been used for bars of 25 mm, then the feasibility of this system should be studied through the bond strength of this lapping joint splice.

In this paper, an experimental study on the strength of different types of bar joints is reported. Test results on main bar joints for PCa structures are compared with those for cast in situ ones. The influence on the strength when one lapping bar with the same section to the main bar is used instead of two bars, is also studied. Test results are compared with the existing equations for spliced bars.

2. SPECIMENS

The test specimens were designed to represent a confined section of PCa members. Figure 1 shows the detailed sections of typical precast specimens. Two sections of specimens were used, one with 4 bars and a section of 450 mm x 700 mm and the other with 3 bars and a section of 350 mm x 700 mm. In both sections, the distance between the bar axis is 100 mm.

Six types of splices were tested in this investigation. Differences among the splices are shown in Fig. 2 and listed in Table 1. Splice types A and B correspond to those used for precast columns, while C and D for precast beams. Generally beams are subjected to unidirectional bending, while columns

*1 Doctoral Degree Program, University of Tsukuba
*2 Undergraduate Student, University of Tsukuba
*3 Technical Research Institute, Kabuki Construction Co. Ltd.
*4 Institute of Engineering Mechanics, University of Tsukuba

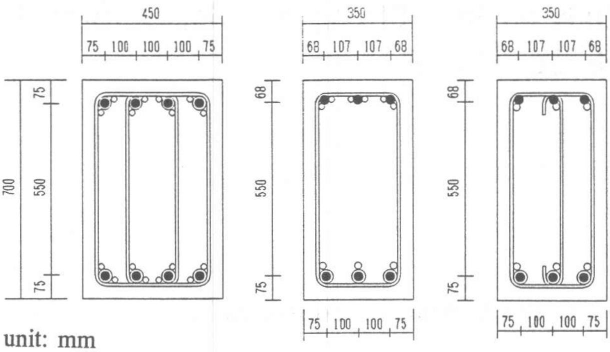

unit: mm

(a) AA-1 (b) EC-10 (c) FC-12

Fig. 1 Section of specimens

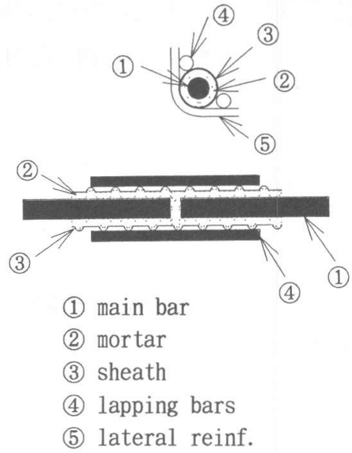

(d) details

Table 1 Differences among specimens

SPECIMEN	SPECIMEN LENGTH (mm)	SECTION (mm)	MAIN BAR	LAPPING BAR	LAPPING LENGTH (mm)	LATERAL REINFORC.
AA-1	1000	450x700	4-D25	2-D19	760	4-D10@100
BB-2						
EA-3						4-D10@150
EB-4						
EA-5						4-D10@200
CC-6	1200			1-D25	1000	4-D10@100
FC-7						4-D10@150
FD-8						
FC-9						4-D10@200
EC-10		350x700	3-D25	2-D19	760	2-D10@150
				1-D25	1000	
DG-11				1-D25	1000	
FC-12						3-D10@150
GD-13						

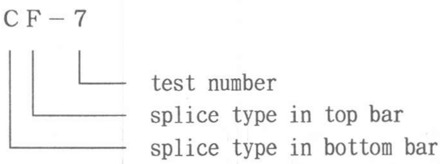

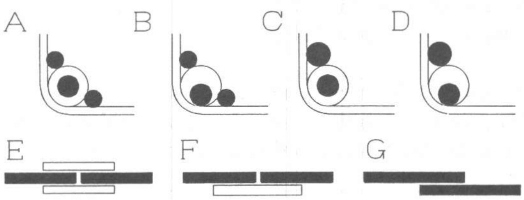

Fig. 2 Types of splice

to bi-directional bending. The length in beams is large enough to allow the splicing of bars with a lapping length longer than those for columns, without reaching the hinge region. In these cases a bar with the same size as the main bar is proposed to be used, represented in this experiment by types C and D. Splice types E to G correspond to top bars of beams. Spliced types E and F were conceived to compare its test results with those of the bars with sheaths. Splice type G is the conventional bar splice used up to the present.

A steel spiral sheath of 42 mm diameter with lug height of 2 mm was used. Also, a cover concrete of 40 mm from the surface to the lateral reinforcement was fixed for all specimens. Each specimen had 4–D10 (SD295A) as lateral reinforcement, except when its influence on the joint strength was tested. As lapping length, 20 times the diameter of the lapping bar, 20d, was considered for all the PCa specimens.

The specimens were cast horizontally. The direction of casting was the basis of naming the upper cast bars as "top bars" and the lower cast ones as "bottom bars". Also, the high strength mortar was grouted horizontally. Concrete was placed at the end of the specimens to seal the sheaths and then mortar was injected by using a pump.

The specified concrete strength for the PCa specimens was Fc= 300 kgf/cm^2 and the specified compressive strength of the grout mortar was 600 kgf/cm^2. For main bars, D25 with specified yield strength of 4000 kgf/cm^2 (SD390), and as lapped bars two bars of D19 (SD390) or one bar of D25 (SD390) were chosen for this investigation. Tables 2, 3 and 4 show the properties of the materials.

Table 2 Properties of concrete

Specimen		Fc (kg/cm^2)	σ_B (kg/cm^2)
AA-1 FC-9 EC-10	1	300	308
	2		322
BB-2 EA-5 GD-11	1		326
	2		308
EA-3 CC-6 FC-12	1		322
	2		308
EB-4 FC-7 GD-13	1		305
	2		293
FD-8	1		215
	2		215

3. TEST APPARATUS AND LOADING HISTORY

The loading arrangement is shown in Fig. 3. Tensile force P was applied horizontally to both ends of each main bar by oil jacks controlled by a load cell. Displacements between both ends of the main bars were also measured.

To obtain the maximum load, monotonic load was applied to all specimens with an increment of 1 tonf until failure. In case of the bottom bars, the maximum load was obtained after the bars almost yielded. The top bars did not yield before bond failure.

Table 3 Properties of mortar

Grout Mortar	Specified (kg/cm^2)	Test (kg/cm^2)
13 days	600	500
28 days		604
78 days		651
98 days		685

The following testing procedure was adopted for two specimens with the same parameter: first the top bar was tested until the specimen was close to failure. Then the bottom bar was tested until it failed, then the bottom bar of the second specimen was tested until the load was close to the maximum load, so after that the top bar was tested until failure. By this testing pattern the authors tried to get good results with the limited number of specimens in each case.

Table 4 Properties of steel

Bar	Grade	σ_y (tf/cm^2)	σ_B (tf/cm^2)	E (tf/cm^2)
D10	SD295A	3.56	5.19	1930
D19	SD390	4.32	6.00	1900
D25		4.31	6.12	1880

4. TEST RESULTS

Relations for all test specimens between lapping lengths, bond stresses, and main stresses at the maximum loads are illustrated in the following figures. These diagrams were deduced by converting applied maximum forces into bond stresses using Eq. (1). Also, bond splitting strengths calculated by the formulas proposed by Fujii–Morita [3], Eq. (2); Orangun–Jirsa–Breen [4], Eq. (3) and Jimenez–White–Gergely [5], Eq. (4) are plotted in every case.

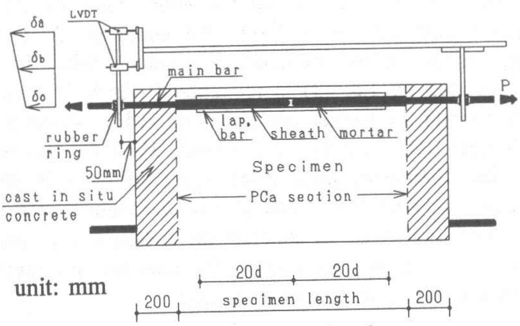

unit: mm

d: diameter of lapping bars

Fig. 3 Loading system

Equation (2) was derived for continuous bars from the bond splitting failure, while Eqs. (3) and (4) were derived for bars with lapping splices. In Eq.(4) the cover of concrete, as well as the concrete strength are dominant parameters, therefore the calculated values obtained from this equation are almost similar because of the same cover of concrete (40 mm).

$$\tau_{exp}=\frac{Pmax}{ls\phi} \cdots\cdots (1)$$

$$\tau_{cm}=(0.307b_i+0.427+24.9\frac{kA_{st}}{sN_t d_b})\sqrt{\sigma_B} \cdots\cdots (2)$$

multiplied by 1.22 for bottom bars

$$\tau_{coj}=(1.2+3\frac{C}{d_b}+50\frac{d_b}{ls}+\frac{A_w\sigma_y}{35.2N_t s d_b})0.265\sqrt{\sigma_B} \cdots (3)$$

divided by 1.3 for top bars

$$\tau_{cji}=\frac{1}{4}(\frac{C\sqrt{\sigma_B}}{0.105d_b+0.0017ls}+0.573\rho_v f_{yt}) \cdots\cdots (4)$$

where:

Pmax: maximum force in the main bar;
ϕ: perimeter of sheath or bar (without sheath);
ls: lapped length;
bi: parameter for the failure of concrete;
k: parameter of the lateral reinforcement;
Ast=Aw: area of lateral reinforcement;
Nt: total number of main bars;
db: diameter of sheath;
$f_{ty}=w\sigma y$: yielding strength of lateral reinforcement;
C: half clear spacing between bars or half available concrete width per bar or splice resisting splitting in the failure plane;
σ_B: concrete cylinder strength;
ρ_v: lateral reinforcement ratio.

The experimental bond strength τ_{exp} and the calculated bond strength (τ_{cm}, τ_{oj}, τ_{ji}) are compared in Figs. 4, 5, and 6. From Fig. 4, a large scatter of the experimental values with respect to the calculated values by Eq. (2) is observed, while some of them agree well with those from that equation. A good agreement of the experimental values with those calculated by Eq. (3) is recognized. As it is above mentioned, the predominant factors in Eq. (4) are the strength and the cover of concrete, while the amount of lateral reinforcement has a small influence in this equation. Therefore, with almost the same concrete strength and cover of concrete the correlation appears as a vertical line for cast in situ bars and for joints using sheaths, with a small scatter.

The forces at which the initial cracks were observed are calculated based on the assumption that

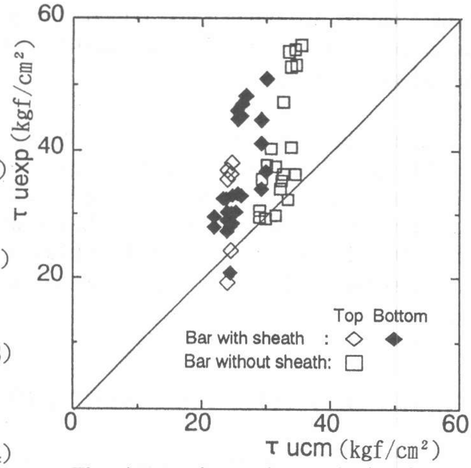

Fig. 4 Experimental vs calculated values using Morita's Eq.

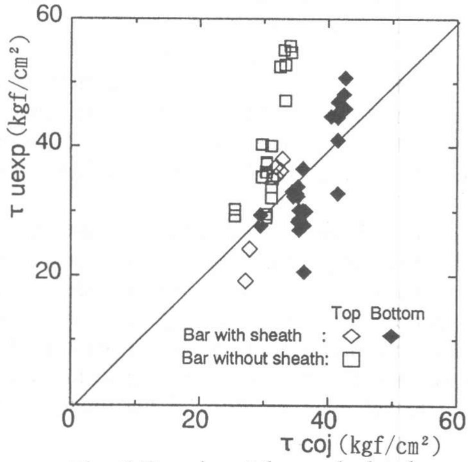

Fig. 5 Experimental vs calculated values using Orangun's Eq.

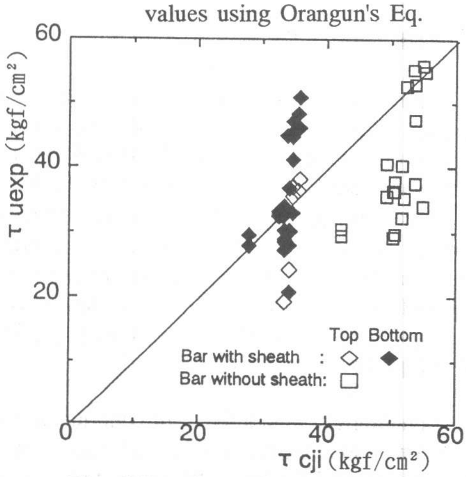

Fig. 6 Experimental vs calculated values using Jimenez's Eq.

plane section remains plane after deformation:

$$P=\frac{BD^2F_b}{D+6e} \cdots\cdots\cdots\cdots (5)$$

where:

P: force in the main bar when the first crack appears;
B,D: width and depth of the specimen;
e: distance from the loaded bar to the neutral axis of the specimen;
F_b: tensile strength of concrete for bending ($1.8\sqrt{Fc}$).

Figure 7 shows the correlation between the calculated and experimental values. Good agreement is observed, even when the tensile force P was applied with an increment of one tonf.

Figures 8 (a) and (b) show the relation between the tensile stress in main bar and average bond stresses in main bar, sheath, lapping bar at the maximum loads for bars lapped with two or one bar, respectively. In terms of the maximum load, a good performance for the splice types A and B are recognized. In Fig. 8 (a), test results from the spliced top bars with sheaths (splice types A, B) show higher values than those spliced bars without sheaths (splice type E), while the same is not recognized for splice type C, as shown in Fig. 8 (b).

Figures 9 (a) and (b) show the comparison between the average maximum loads for the top and bottom bars, respectively. Here, no difference between the maximum loads of the bottom bars is recognized for splice types A, B, C and D. Therefore, no influence of the eccentricity of the bar with respect to the sheath axis is recognized. The splice types A and B for top bars show better performance than the other types of splicing. These test results show that if one main bar is spliced with two lapping bars instead of one lapping bar, a better performance of the spliced joint can be expected.

In terms of bond strength, it is remarkable to say that the bottom bars with

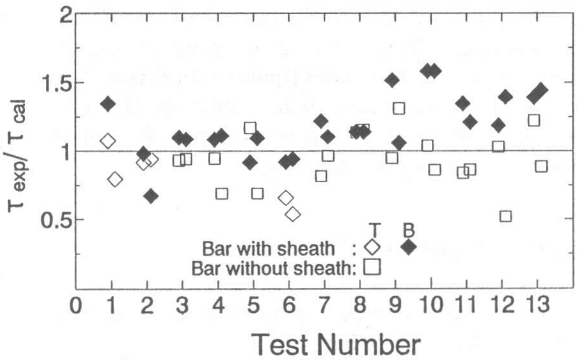

Fig. 7 Correlation between the experimental and calculated forces for bending cracks

σ : tensile stress in main bar (tf/cm²)
τb : bond stress in main bar (kgf/cm²)
τs : bond stress in sheath (kgf/cm²)
τlb: bond stress in lapping bars (kgf/cm²)

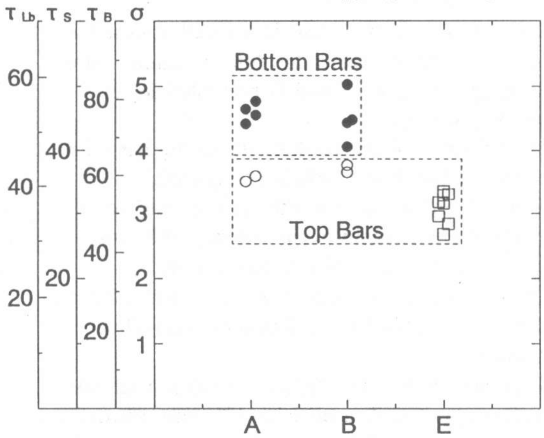

(a) Splices with two lapping bars

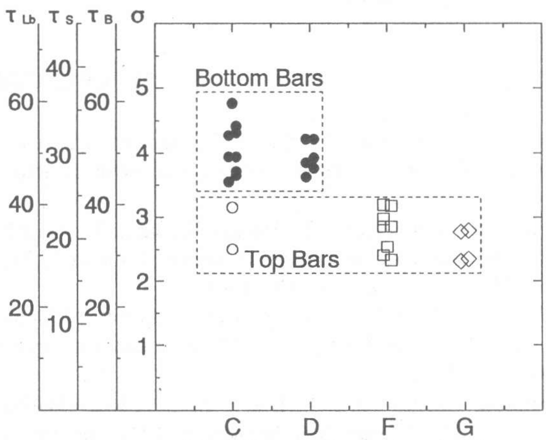

(b) Splices with one lapping bar

Fig. 8 Relation between joint strength and number of lapping bars sheaths presented almost the same bond strength as the top bars without sheaths as shown in Fig. 8. Furthermore, specimen with lapping splice types A, B and lateral reinforcement with a pitch of 100 mm, showed a better performance in either the top or bottom bars than other specimens.

5. CONCLUSIONS

From the foregoing discussions, the following conclusions can be obtained.

1) The load for the initial bending cracks can be predicted with good accuracy based on the assumption that plane section remains plane after deformation.
2) A better performance for the bottom bars than for the top bars is recognized.
3) Splice types A, B, C and D showed almost the same strength for either the top or bottom bars, while splice Types F and G presented lower strength than C.
4) No influence of the eccentricity of the bar with respect to the sheath axis is recognized.
5) A better performance of the spliced joint could be expected if one main bar is spliced with two lapping bars instead of one lapping bar.
6) The test results showed good agreement with the calculated values by the Orangun–Jirsa–Breen equation.
7) Specimen with splice types A or B and lateral reinforcement with a pitch of 100 mm, showed a better performance in either the top or bottom bars than other specimens.

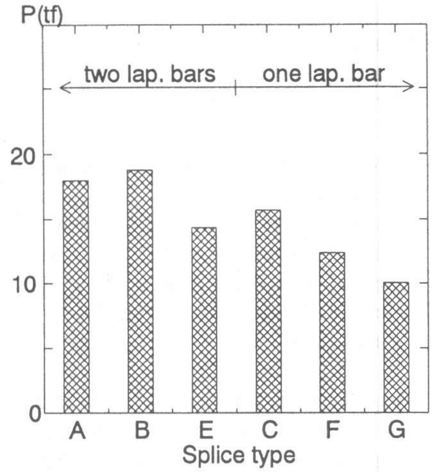

(a) Top bars

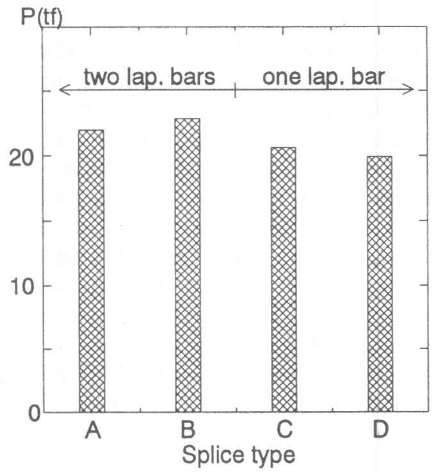

(b) Bottom bars

Fig. 9 Comparison of the average maximum load

REFERENCES

1.Imai, H.; Yamaguchi, T.; Yanez, R., "Bond Performance of a Lapping Joint Developed for Precast Concrete Columns", Proceedings of The Japan Concrete Institute, Vol. 13, No 2, 1991, pp. 1063–1068.

2.Yanez, R.; Yamaguchi, T.; Hibino K.; Imai, H., "An Experimental Study on the Strength of a Proposed Bar Joint for Precast Concrete Columns", Proceedings of The Japan Concrete Institute, Vol. 14, No 2, 1992, pp. 999–1004.

3.Fujii, S.; Morita, S., "Splitting Bond Capacity of Deformed Bars (Part 2), A Proposed Ultimate Strength Equation for Splitting Bond Failure (in Japanese)", Transactions of AIJ, No. 324, Feb. 1983, pp. 45–53.

4.Orangun, C.O.; Jirsa, J.O.; Breen, J.E., "A Reevaluation of Test Data on Development Length and Splices", ACI Journal, Vol 74, March, 1977, pp. 114–122.

5.Jimenez, R.; White, N.; Gergely, P., "Bond and Dowel Capacities of Reinforced Concrete", ACI JOURNAL, Proceedings V.76, No. 1, January 1979, pp. 73–92.